

dc3dm is a free open source software (FOSS) package that efficiently forms and applies the linear operator relating quasistatic dislocation and traction components on a nonuniformly discretized rectangular planar fault in a homogeneous elastic (HE) half space. This linear operator implements what is called the displacement discontinuity method (DDM).

The key properties of dc3dm and the algorithms it implements are: 1. The mesh can be nonuniform. 2. Work and memory scale roughly linearly in the number of elements (rather than quadratically). 3. The order of accuracy on a nonuniform (or uniform) mesh is the same as that of the standard method on a uniform mesh.

Property 2 is achieved using my FOSS package hmmpv [Bradley, 2011].

A nonuniform mesh (property 1) is natural for some problems. For example, in a rate-state friction simulation, nucleation length, and so required element size, scales reciprocally with effective normal stress. For example, an 8x difference in normal stress yields a 64x difference (8x in each fault-parallel direction) in number of required elements per unit area. A simulation can take advantage of factors of this order for speedup relative to using a uniform mesh.

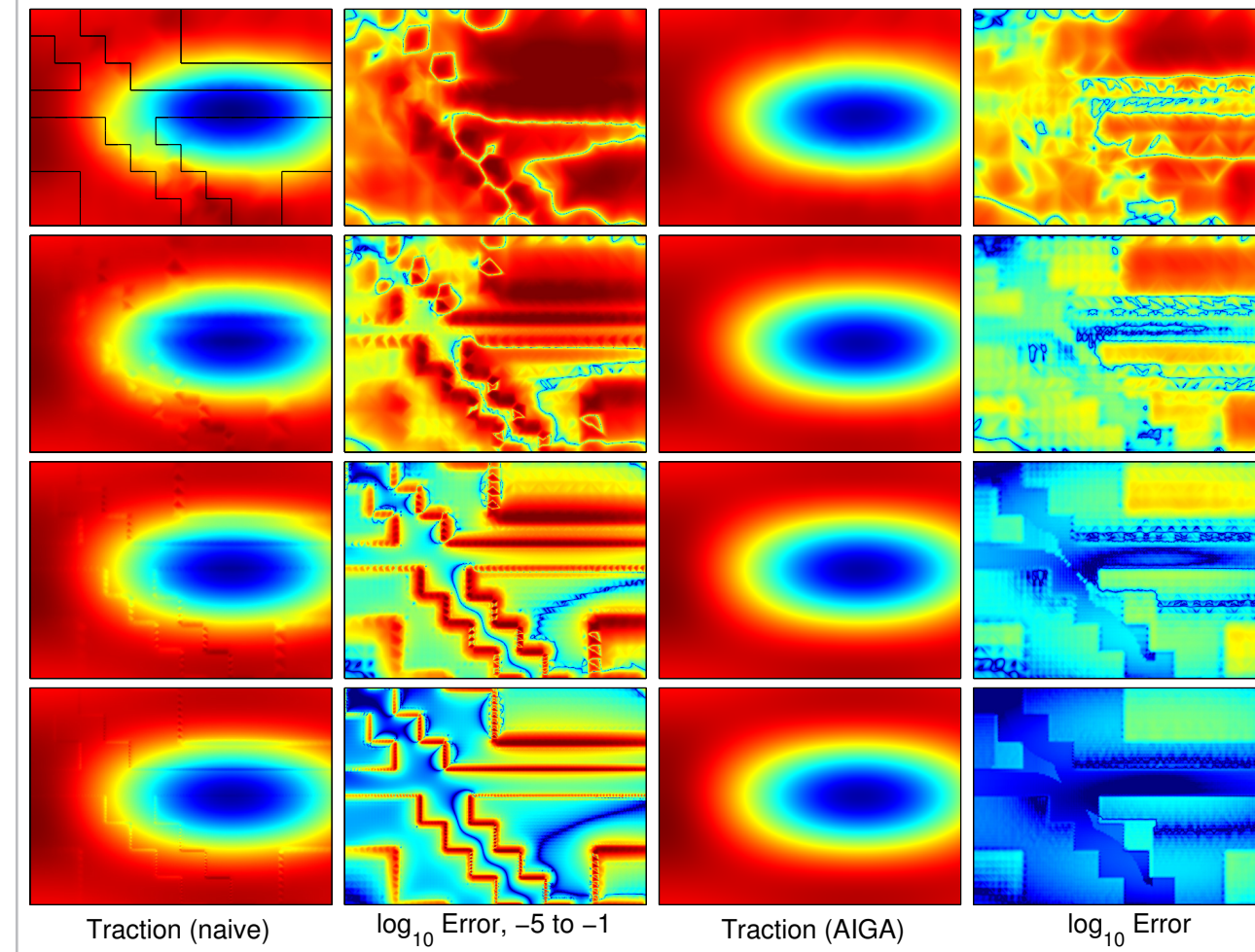


Figure 1: Tractions and pointwise absolute errors (relative to maximum traction magnitude) for the naive (left two columns) and AIGA methods (right) applied to the strike-strike GF for the problem described in Section 4. From top to bottom, the level of refinement increases successively by 2. The naive method causes errors where adjacent elements differ in size (outlined by black lines in the top-left image); peak magnitude of the error stays approximately constant with refinement. Color scales are the same in respectively columns 1 and 3, and 2 and 4. Images are zoomed to a region of interest.

## 1. hmmpv: A PACKAGE TO COMPRESS MATRICES HAVING LOW-RANK STRUCTURE

Let a fault be discretized uniformly into  $N = N_x N_y$  patches. In a whole space, the 2D FFT can be used to calculate stress from slip in  $O(N \log N)$  work. In a half space, the FFT can be used in the along-strike direction for  $O(N_x^2 N_y \log N_y)$  work. Without a speedup method (e.g. the FFT), the work would be  $O(N^3)$  in both cases. The DFT can be implemented by a matrix-vector product (MVP) with a completely dense matrix. The FFT takes advantage of *exact low-rank structure*.

For a nonuniformly discretized or nonplanar fault, the FFT cannot be applied. A class of methods including the fast multipole method, Barnes-Hut, and hierarchical matrices (H-matrices [Bebendorf, 2008]) are instead applicable. These methods take advantage of *off-diagonal block* (for an appropriate permutation) *approximate low-rank structure*. A block  $B \otimes U V^T$ , with columns( $U$ )  $\ll$  min(rows( $B$ )), columns( $B$ )). Work is  $O(N \log N)$  on the uniform mesh in this discussion; it is asymptotically  $N_d \times \log N_s / \log N$  faster than an along-strike FFT.

hmmpv is a package to *form* and *apply* (by an MVP) an H-

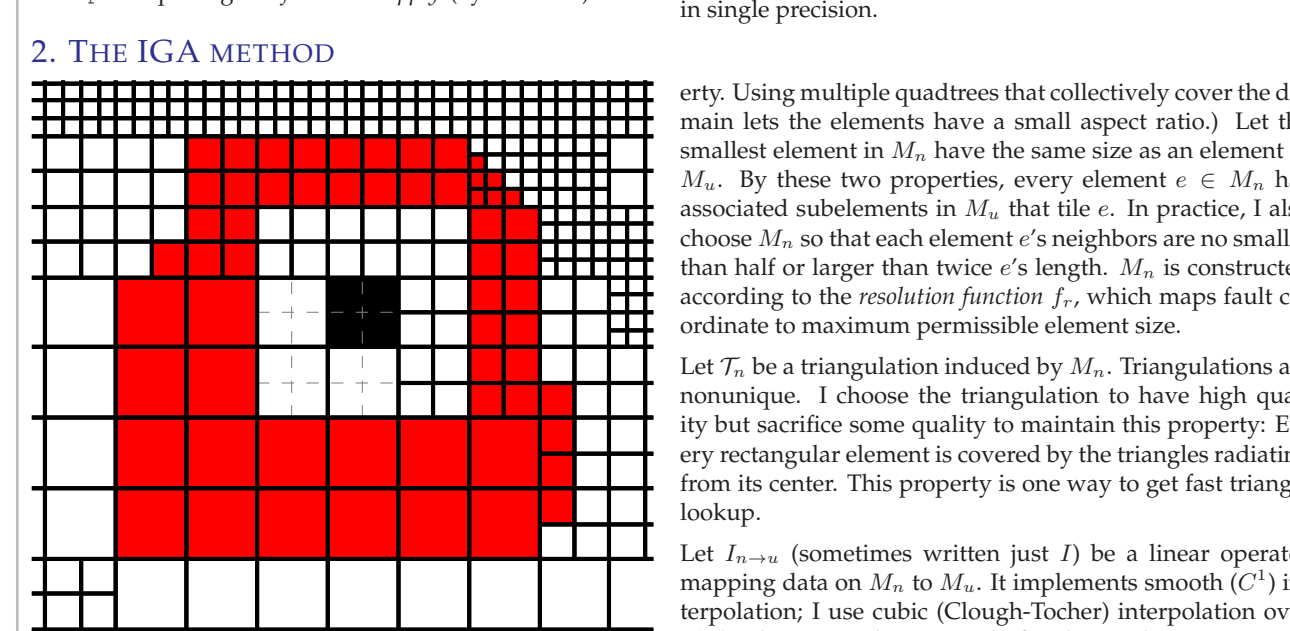


Figure 2: (left)  $\log_{10}$  Number of structural nonzeros in H-matrix vs.  $\log_{10} N$ , with three growth rates for reference. (right) H-matrix file size (metadata + coefficients) vs.  $\log_{10} N$ , compared with the uncompressed matrix size in single precision.

erty. Using multiple quadtrees that collectively cover the domain lets the elements have a small aspect ratio. Let the smallest element in  $M_n$  have the same size as an element in  $M_u$ . By these two properties, every element  $e \in M_n$  has associated subelements in  $M_u$  that file  $e$ . In practice, I also choose  $M_n$  so that each element  $e$ 's neighbors are no smaller than half or larger than twice  $e$ 's length.  $M_n$  is constructed according to the resolution function  $f_r$ , which maps fault coordinate to maximum permissible element size.

Let  $T_n$  be a triangulation induced by  $M_n$ . Triangulations are nonunique. I choose the triangulation to have high quality but sacrifice some quality to maintain this property: Every rectangular element is covered by the triangles radiating from its center. This property is one way to get fast triangle lookup.

Let  $I_{n-u}$  (sometimes written just  $I$ ) be a linear operator mapping data on  $M_n$  to  $M_u$ . It implements smooth ( $C^1$ ) interpolation; I use cubic (Clough-Tocher) interpolation over  $T_n$  (with certain choices made for the gradient estimates). This method has order of accuracy (OOA) greater than 2. (See Section 4 for more on OOA.)

Let  $A_{n-u}$  (or just  $A$ ) be a linear operator mapping data on  $M_u$  to  $M_n$ . Let  $e \in M_n$ , be tiled by  $E \subset M_u$ . A averages values at the centers of  $f \in E$  to the center of  $e$ . Because the center of  $e$  is also the center of  $E$ , averaging is equivalent to a linear fit followed by interpolation. Hence  $A$  has OOA 2. Finally, let  $G_u$  be the DDMu operator.

These three linear operators together implement exact IGA (EIGA):  $G_u \equiv A_{n-u} I_n I_{n-u}$ .

Let  $M_n$  be a nonuniform mesh having the following property: Each element must tile each element larger than itself. (A mesh generated by a family of quadtrees has this prop-

erty.) EIGA has the undesirable property that its computational complexity is determined by the smallest element in  $M_n$ ; this element induces the mesh  $M_u$  for which the three matrices  $A$ ,  $G_u$ , and  $I$  must be computed. Approximate IGA (AIGA) uses an additional idea to solve this problem. Define a parameter  $\delta_r$  that sets receiver neighborhood size. It is a number between 0 (no neighborhood; in fact, identical to the naive method) and a problem-dependent value at which EIGA is reached.

dc3dm implements AIGA; DDMu is recovered with certain choices, so dc3dm can also be used simply as a convenient layer on top of hmmpv for problems involving planar rectangular faults. Matrices for all nine source-receiver dislocation-traction pairs and linear combinations of dislocations and tractions, respectively, can be calculated.

Boundary conditions (BC) can be periodic in the surface-parallel direction (in both directions if the GF is for a whole space), velocity, and free surface. Periodicity is approximate; the domain is repeated periodically a finite number of times. For a given source-receiver pair, the periodically repeated source nearest the receiver is used as the primary source, and then a specified number of layers are constructed.

Importantly, IGA's order of accuracy on a nonuniform mesh is the same as DDMu's on a uniform one (property 3).

The latest version of hmmpv and the new dc3dm are available at

[pangea.stanford.edu/research/CDFM/software](http://pangea.stanford.edu/research/CDFM/software)

In the following, colors refer to Fig. 3. Full IGA source-

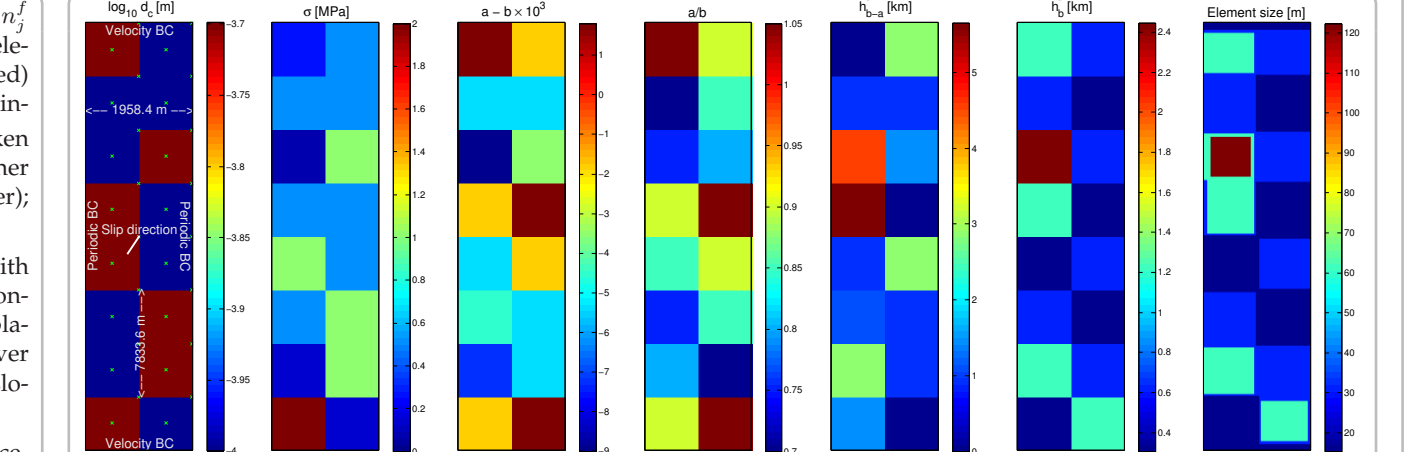


Figure 3: A nonuniform mesh with an example of a receiver's neighborhood. The black element is the receiver. Gray dashed lines show subelements of type-1 source elements. Subelements are as small as the smallest type-1 element.

Subelements are as small as the smallest type-1 element.

Type-2 elements, which help with interpolation but are not themselves subdivided, are red. Type-3 elements, which act on the receiver simply, are white.

Exact IGA. Let  $M_n$  be a uniform mesh. DDMu constructs a matrix  $G_u$  to relate traction and slip by  $\tau_u = G_u s_u$ .

Let  $M_n$  be a nonuniform mesh having the following property: Each element must tile each element larger than itself. (A mesh generated by a family of quadtrees has this prop-

erty.) EIGA has the undesirable property that its computational complexity is determined by the smallest element in  $M_n$ ; this element induces the mesh  $M_u$  for which the three matrices  $A$ ,  $G_u$ , and  $I$  must be computed.

Approximate IGA (AIGA) uses an additional idea to solve this problem. Define a parameter  $\delta_r$  that sets receiver neighborhood size. It is a number between 0 (no neighborhood; in fact, identical to the naive method) and a problem-dependent value at which EIGA is reached.

dc3dm implements AIGA; DDMu is recovered with certain choices, so dc3dm can also be used simply as a convenient layer on top of hmmpv for problems involving planar rectangular faults. Matrices for all nine source-receiver dislocation-traction pairs and linear combinations of dislocations and tractions, respectively, can be calculated.

Boundary conditions (BC) can be periodic in the surface-parallel direction (in both directions if the GF is for a whole space), velocity, and free surface. Periodicity is approximate; the domain is repeated periodically a finite number of times. For a given source-receiver pair, the periodically repeated source nearest the receiver is used as the primary source, and then a specified number of layers are constructed.

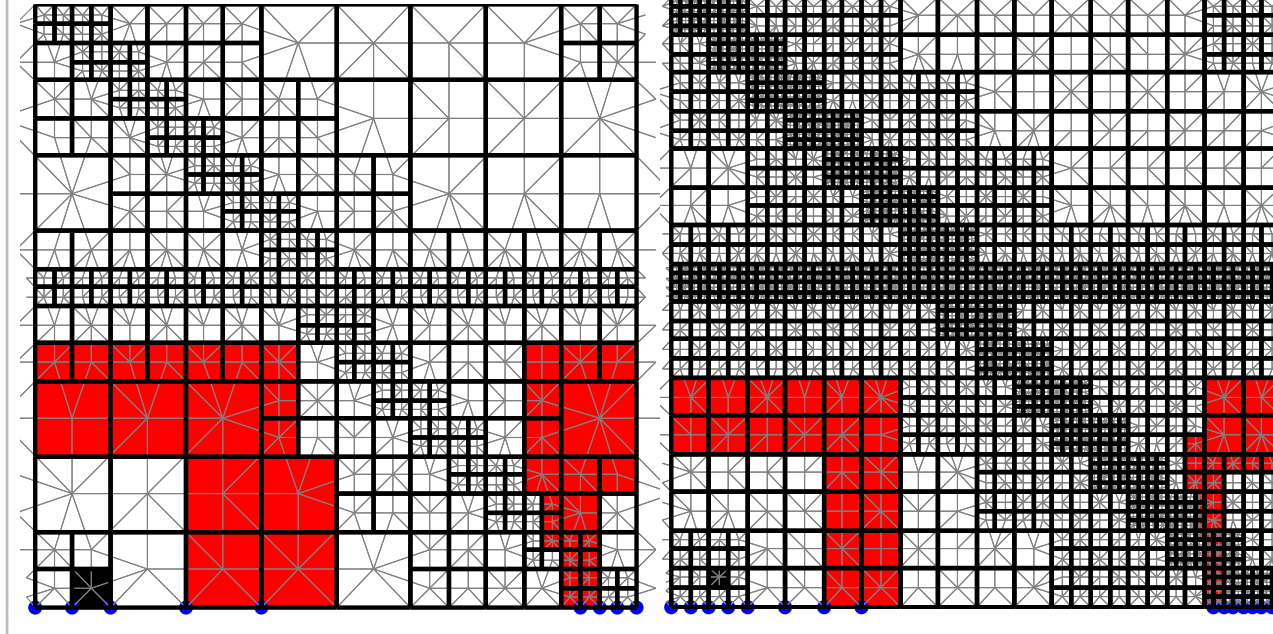
Importantly, IGA's order of accuracy on a nonuniform mesh is the same as DDMu's on a uniform one (property 3).

The latest version of hmmpv and the new dc3dm are available at

[pangea.stanford.edu/research/CDFM/software](http://pangea.stanford.edu/research/CDFM/software)

In the following, colors refer to Fig. 3. Full IGA source-

## 4. CONVERGENCE ANALYSIS



Analysis of the DDMu shows that its OOA is 2 for the strike-strike, dip-dip, tensile-normal, strike-normal, dip-normal, tensile-strike, and tensile-dip source-receiver GFs and 1 for strike-dip and dip-strike. The lower OOA in the final two cases results from the self-interaction calculation for a term of the form  $1/r$ .

Because the operators  $I_{n-u}$  and  $A_{n-u}$  have OOA at least 2 and the range of  $I_{n-u}$  is  $C^1$ , EIGA inherits the OOA of DDMu or the opposite is arbitrary, as the mesh and test slip function are chosen independently; only the order of accuracy (error curve slope) matters. The mesh is chosen to be interesting, and the test slip function is chosen to permit converged results without refining the mesh too many levels and to respect the BCs. Fig. 4 shows the level-0 and 1 meshes.

$\delta_r$ , at level  $i$ , is chosen as  $\delta_r^i = (2/(2\delta_r^{i-1}) - 1)/2$ . This choice implements the following rule. If  $e \in E$ , where  $E$  at level  $j$  is the set of elements that tile  $e$  at level  $i < j$ , then the area of the neighborhoods around  $e$  and  $f \in E$  must be the same (in the limit of refinement); at finite refinement, areas are almost certainly slightly different.

A suite of empirical convergence tests (ECT) is used as one test of dc3dm. The suite includes every corner combination of BCs and source-receiver component. Fig. 5 shows results for a subset of the ECT for the most interesting combination of BCs and strike-(strike, normal, dip) source-receiver GFs. Relative error is with respect to the solution of DDMu on a very fine mesh.

$\delta_r$ , at level  $i$ , is chosen as  $\delta_r^i = (2/(2\delta_r^{i-1}) - 1)/2$ . This choice implements the following rule. If  $e \in E$ , where  $E$  at level  $j$  is the set of elements that tile  $e$  at level  $i < j$ , then the area of the neighborhoods around  $e$  and  $f \in E$  must be the same (in the limit of refinement); at finite refinement, areas are almost certainly slightly different.

Coarse solutions are mapped to the fine mesh using IGA's interpolant. Whether AIGA is more accurate than DDMu or the opposite is arbitrary, as the mesh and test slip function are chosen independently; only the order of accuracy (error curve slope) matters. The mesh is chosen to be interesting, and the test slip function is chosen to permit converged results without refining the mesh too many levels and to respect the BCs. Fig. 4 shows the level-0 and 1 meshes.

$\delta_r$ , at level  $i$ , is chosen as  $\delta_r^i = (2/(2\delta_r^{i-1}) - 1)/2$ . This choice implements the following rule. If  $e \in E$ , where  $E$  at level  $j$  is the set of elements that tile  $e$  at level  $i < j$ , then the area of the neighborhoods around  $e$  and  $f \in E$  must be the same (in the limit of refinement); at finite refinement, areas are almost certainly slightly different.

A base mesh is created for DDMu and AIGA at refinement level 0. At level  $i$ , each base element is divided into  $4^i$  ele-

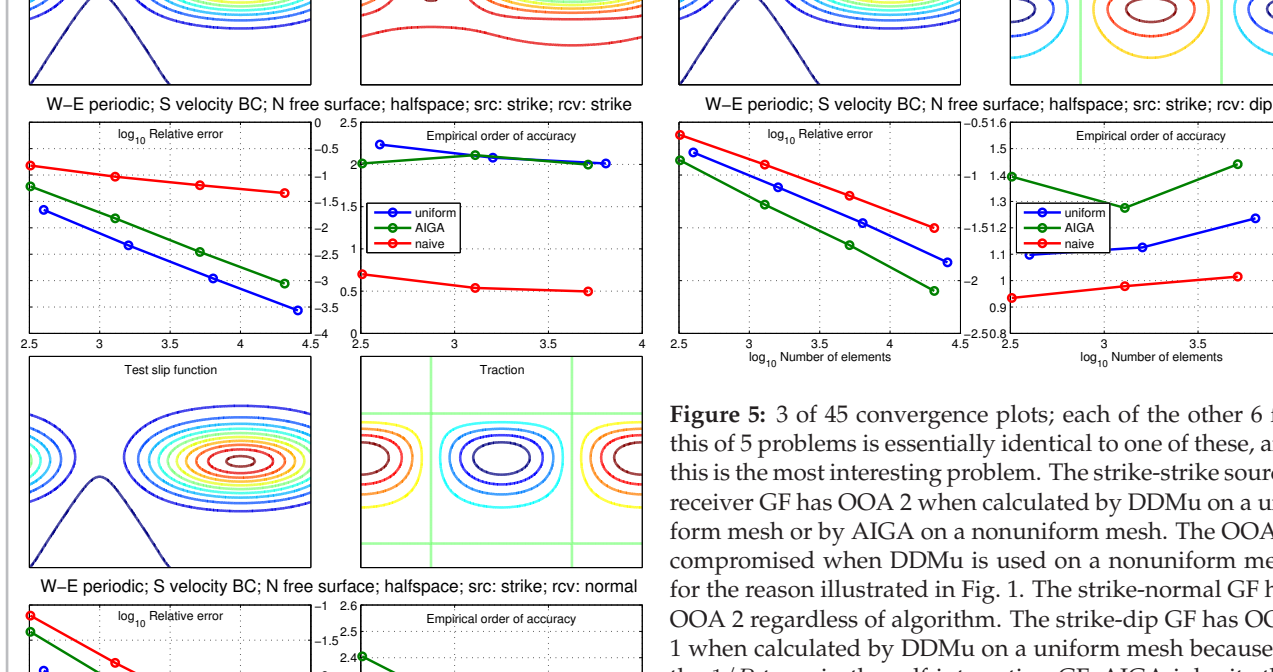


Figure 5: 3 of 45 convergence plots; each of the other 6 for this of 5 problems is essentially identical to one of these, and this is the most interesting problem. The strike-strike source-receiver GF has OOA 2 when calculated by DDMu on a uniform mesh or by AIGA on a nonuniform mesh. The OOA is compromised when DDMu is used on a nonuniform mesh for the reason illustrated in Fig. 1. The strike-normal GF has OOA 1 regardless of algorithm. The strike-dip GF has OOA 1 when calculated by DDMu on a uniform mesh because of the  $1/R$  term in the self-interaction GF. AIGA inherits this compromised OOA. In fact, I think AIGA can improve the OOA to nearly 2, but I have not worked out an efficient way to do so yet, and it may be a low priority in the short term.

## 5. TIME-DEPENDENT PROBLEM 1: A TEST WITH DISCONTINUOUS PROPERTIES

In quasistatic (or quasidynamic) state-space friction simulations, the resolution function  $f_r$  should be a function of fault properties. One such function is  $f_r = \mu \alpha / (1 - \nu) d_c / (\sigma b)$ , where  $\mu$  is the shear modulus,  $\nu$  is Poisson's ratio,  $b$  is the constant multiplying the state term in state-space friction,  $\sigma$  is the effective normal stress,  $d_c$  is the characteristic slip length as  $d_c / (b\sigma)$ , and  $\alpha$  is a constant  $\lesssim 1/5$ . The motivation for this particular  $f_r$  is that rupture tip length scales as  $d_c / (b\sigma)$  for the aging evolution law and that quantity times one depends on slip speed and background values for the slip law. Rupture tips must be well resolved in simulations.

Finally, let  $G_u$  be the DDMu operator.

These three linear operators together implement exact IGA (EIGA):  $G_u \equiv A_{n-u} I_n I_{n-u}$ .

Let  $M_n$  be a nonuniform mesh having the following property:

Each element must tile each element larger than itself. (A mesh generated by a family of quadtrees has this prop-

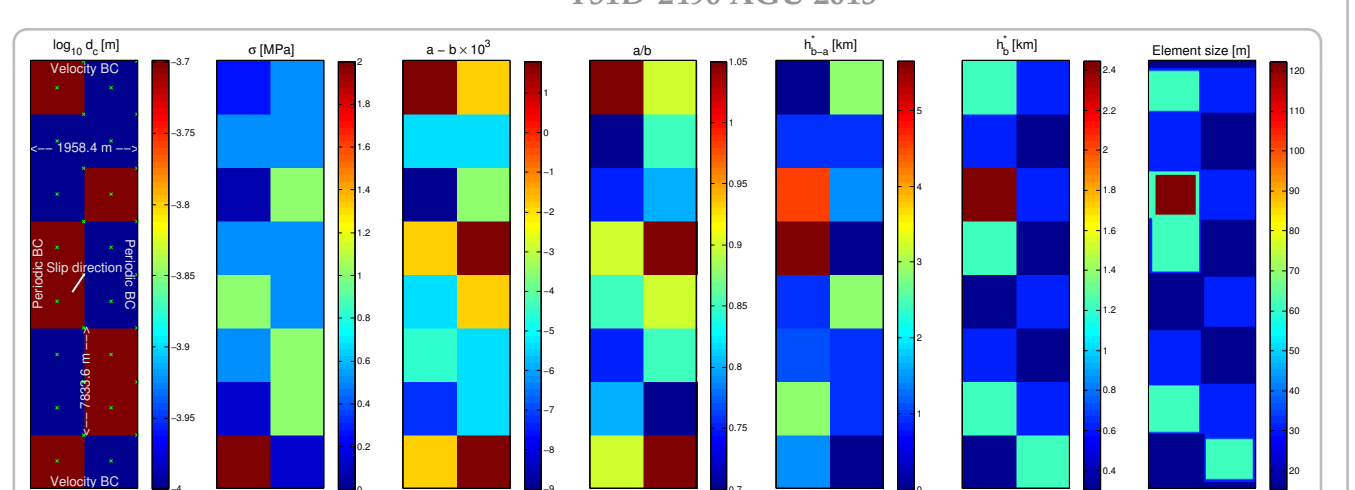


Figure 6: Time-dependent problem 1 setup: properties, critical lengths, and element sizes. This problem has 16 squares, each having different properties. Properties change discontinuously at the edge of each square.

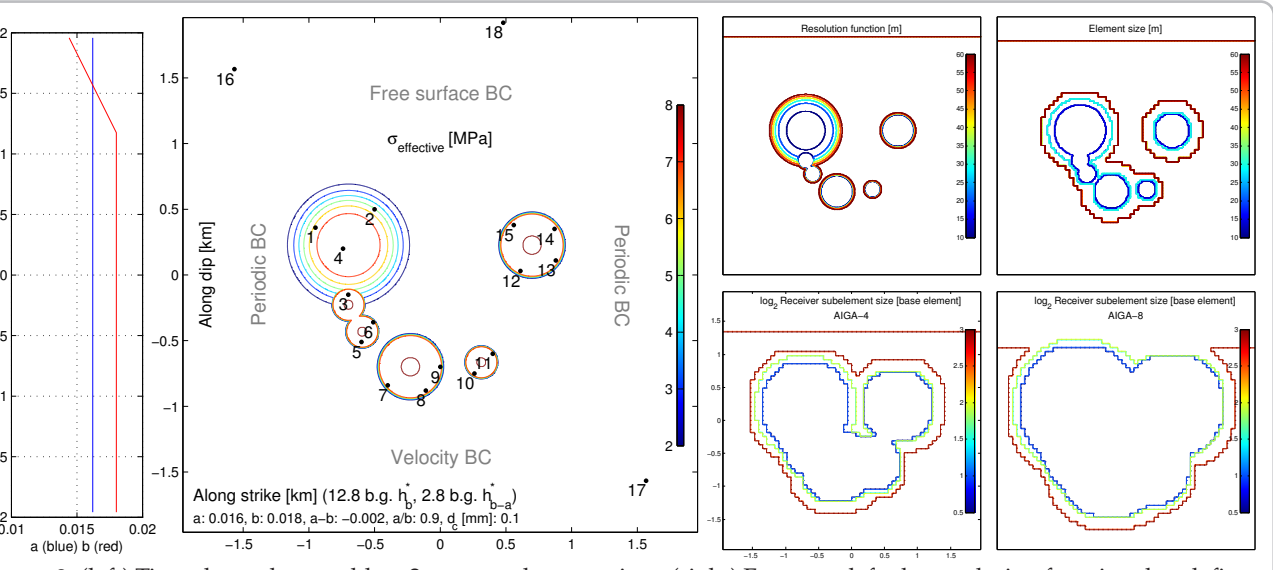


Figure 7: (left) Time-dependent problem 1 setup and trace points. (right) From top-left, the resolution function that defines the mesh, and receiver subelement size for  $\delta_r = 2, 4, 8$ .

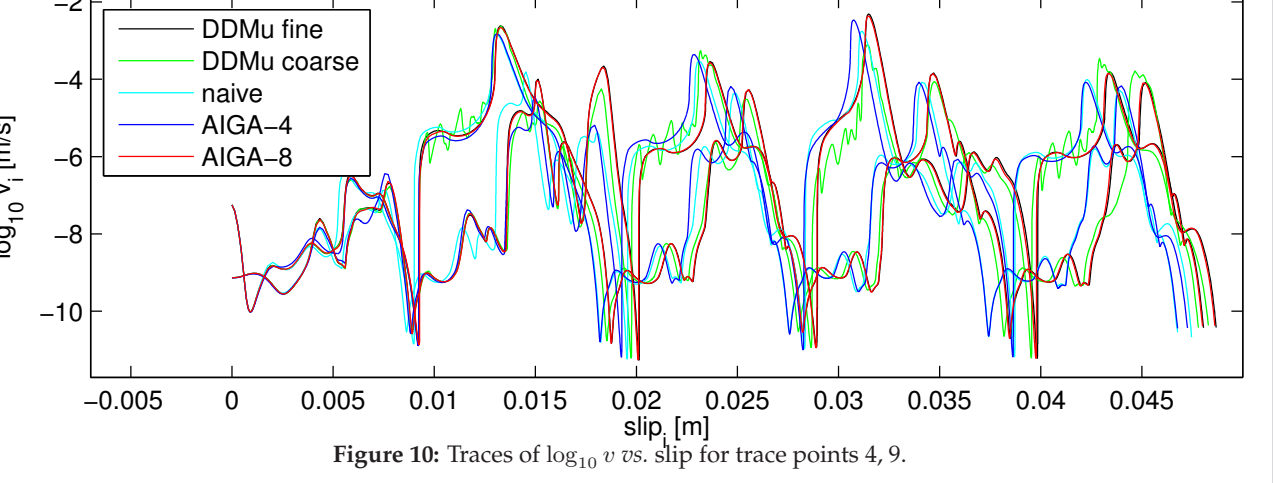


Figure 10: Traces of  $\log_{10} v$  vs. slip for trace points 4, 9.

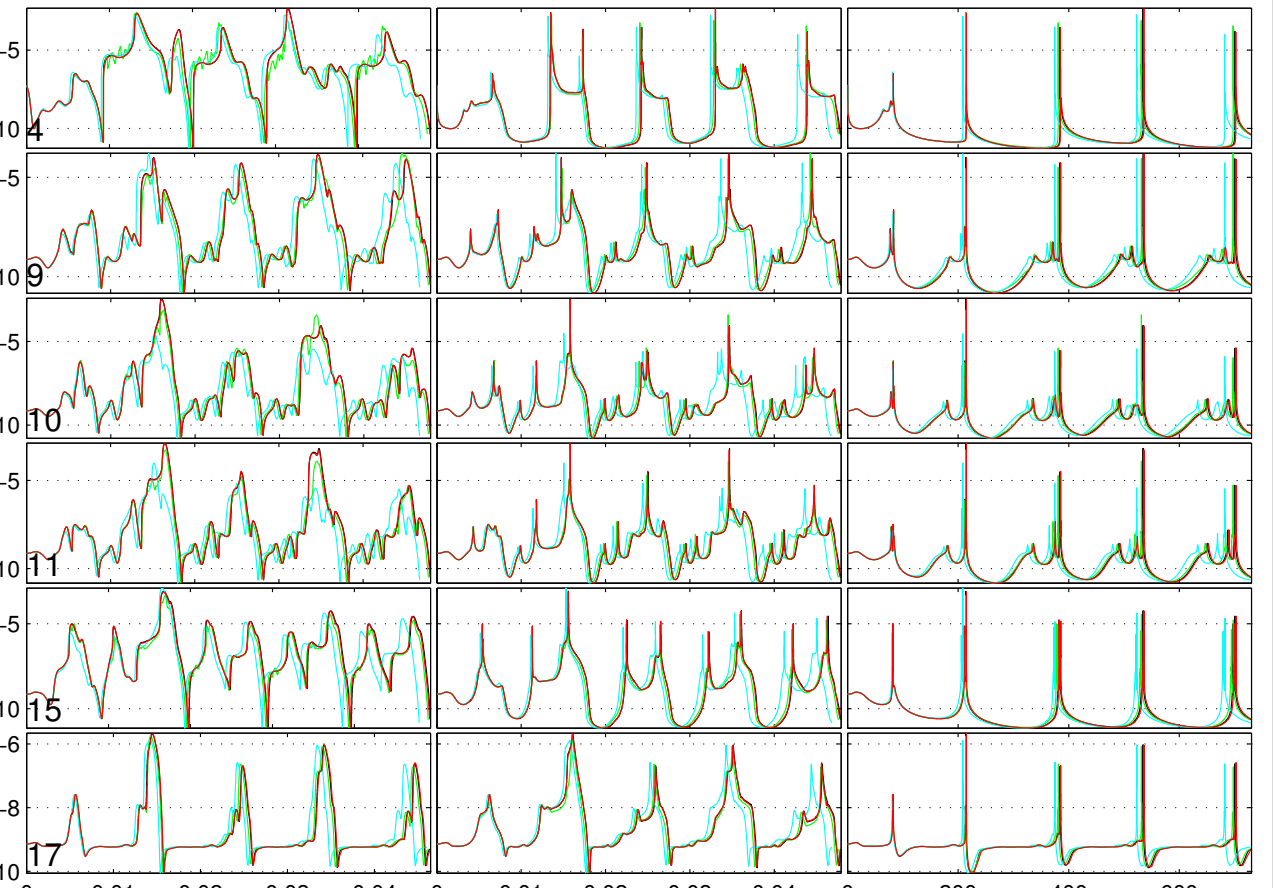


Figure 11: Traces:  $\log_{10} v$  vs. average slip on the fault, and time. Colors are as in Fig. 10.

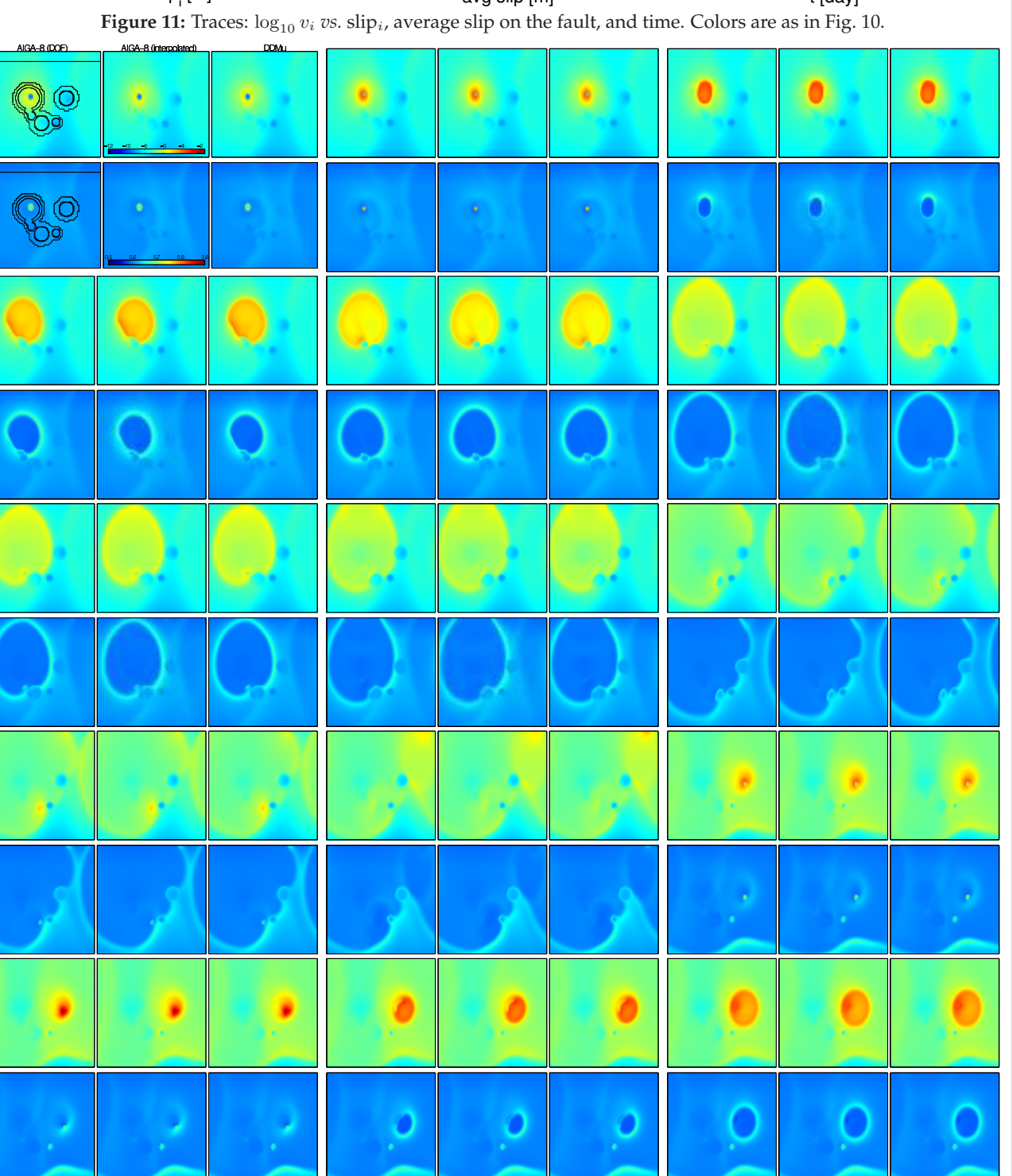


Figure 12: 15 snapshots, with six images each, of  $\log_{10} v$  (top) and friction coefficient (bottom). In each snapshot: (left) AIGA-8 solution at mesh resolution and (middle) interpolated to the uniform mesh; (right) DDMu solution on the uniform mesh. Middle and right images are in close agreement.

Three meshes are used: (i) a uniform mesh with element size  $e_s$ , (ii) a nonuniform mesh with smallest element size  $e_s$  and  $N$  elements, and (iii) a uniform mesh with  $\sqrt{N}$  elements.

Multiple simulations are run: DDMu on (i) ('DDMu fine'), DDMu on (ii) ('DDMu coarse'), DDMu on (iii) ('naive'), and AIGA with  $\delta_r = 4, 8$ .